

1. 학회 포스터

Welcome to the
2015 IEEE Photonics Conference, 28th Annual Conference of the IEEE Photonics Society
4 - 8 October 2015
 Hyatt Regency Reston,
 Reston, Virginia USA

Plenary Speaker
 David A.B. Miller
 Stanford University, USA

2. 학회 프로그램

TUESDAY, 6 OCTOBER 2015

● Indicates a recorded session

Registration & Speaker Check-in Hours: 8:00 AM – 5:00 PM in Grand Ballroom									
Grand Ballroom A	Grand Ballroom B	Grand Ballroom C	Lake Audubon	Grand Ballroom E	Grand Ballroom F	Grand Ballroom G	Lake Anne	Grand Ballroom D	Lake Thoreau
8:30-10:00am TuA1 PSS 1 Group IV APDs J. Campbell	8:30-9:45am TuB1 NLUO 1 Few Optical Cycle and Fiber Lasers M. Khajavikhan	8:30-9:45am TuC1 MWP 3 Analog Photonic Signal Processing R. Logan	8:30-10:00am TuD1 OMND 5 Microresonator Frequency Combs M. Sumetsky	8:30-10:00am TuE1 SL 4 High Power and Visible Lasers P. Crump	8:30-10:00AM TuF1 PIP 3 Device Integration K. Lawniczuk	8:30-10:00am TuG1 OC 5 Datacom & PON Y. Jung	8:30-10:00am TuH1 NANO 4 Nanophotonic Devices I K. Aydin	8:30-10:00am TuI1 OFT 1 SDM and Few Mode Fibers R. Ryf	
EXHIBITS & COFFEE BREAK 10:00 AM - 10:30 AM Regency Ballroom									
10:30-12:00pm TuA2 PSS 2 Group IV Infrared Detectors E. Duerr	10:30-12:00pm TuB2 NLUO 2 Lasers, Oscillators and Amplifiers J. Khurgin	10:30-11:45am TuC2 MWP 4 Detectors & Sensors F. Quinlan	10:30-12:00pm TuD2 OMND 6 Microlasers A. Matsko	10:30-12:00pm TuE2 SL 5 Nitride-based Lasers W. Zhou	10:30-12:00pm TuF2 PIP TUT J. MARSH P. Morton	10:30-12:00pm TuG2 OI 1 Optical Interconnects I E. Johnson	10:30-12:00pm TuH2 NANO 5 Light-Matter Interactions A. Yanik	10:30-12:00pm TuI2 OFT 2 Novel Optical Fibers and Waveguides M. Li	10:30-12:00pm TuJ2 Special Symposium SMLA 1 A. Ramdane
12:00 PM – 1:30 PM LUNCH (on own)									
1:30-2:45pm TuA3 BIO 5 Brillouin Microscopy and Novel Biophotonics M. Gora	1:30-2:45pm TuB3 NLUO 3 Light Guiding, Frequency Comb and Imaging L. Razzari	1:30-3:00pm TuC3 MWP TUT J. CAMPBELL E. Adles & V. Urick	1:30-3:15pm TuD3 OMND 7 Innovative Nanoresonators E. Ben-Bassat	1:30-3:00pm TuE3 SL 6 VCSEL G. Huyet	1:30-3:00pm TuF3 PIP 4 Photonic Integration J. Marsh	1:30-3:00pm TuG3 OI 2 Optical Interconnects II TBD	1:30-3:15pm TuH3 NANO 6 2D Materials N. Yu		1:30-3:00pm TuJ3 Special Symposium SMLA 2 D. Bimberg
EXHIBITS & COFFEE BREAK 3:00 PM - 3:30 PM Regency Ballroom									
3:30 PM – 5:00 PM Plenary Session I - TuI4 Grand Ballroom D Session Chair: Martin Dawson, <i>University of Strathclyde, UK</i> 3:30 - 4:15pm Tailoring Photons, Nader Engheta, <i>University of Pennsylvania, USA</i> 4:15 - 5:00pm Arbitrary Optics – Novel Nanophotonic and Self-adapting Optoelectronic Systems, David A.B. Miller, <i>Stanford University, USA</i>									
5:30 PM – 6:30 PM WOMEN IN PHOTONICS RECEPTION All attendees welcome to attend Regency Ballroom Session Chair: Dalma Novak, <i>Pharad LLC., USA</i>									

12:00 PM - 1:30 PM Lunch Break

10:30 AM - 12:00 PM

Session TuG2: Optical Interconnects I

Session Chair: Eric Johnson, Clemson University, USA

H. Jung

이진

TuG2.1 10:30 AM - 11:00 AM (Invited)

Can Integrated Photonics Technology Transform Datacenters?, M. Haney, US Department of Energy, USA

TuG2.2 11:00 AM - 11:30 AM (Invited)

TBD, D. Plant, McGill University, Canada

TuG2.3 11:30 AM - 11:45 AM

Towards MZI modulator in GeOI and SOI waveguide platforms for Mid-InfraRed wavelengths, M. Rouified, NTU, Nanyang Street, Singapore, T. Hu, C. G. Littlejohns, NTU, Nanyang, Singapore, C. Liu, Temasek Lab-NTU, Nanyang, Singapore and H. Wang, NTU, Nanyang, Singapore

Silicon-On-Insulator and Germanium-On-Insulator are both promising waveguide platforms for the mid-infrared wavelength of 2 μm . Here, we report the design of passive and active devices including multimode interference couplers (MMI) and MZI modulators built on both platforms.

TuG2.4 11:45 AM - 12:00 PM

A High-Speed CMOS Integrated Optical Receiver with an Under-Damped TIA, H. Jung, Yonsei University, Seoul, Korea

We present a CMOS integrated optical receiver with under-damped TIA and CMOS APD. The under-damped TIA compensates bandwidth limitation of CMOS APD. We demonstrate PRBS operation with less than 10⁻¹² BER. The receiver has core size of 0.024 mm² and power consumption of 13.7 mW.

12:00 PM - 1:30 PM Lunch Break

A High-Speed CMOS Integrated Optical Receiver With an Under-Damped TIA

Hyun-Yong Jung, *Student Member, IEEE*, Jeong-Min Lee, *Student Member, IEEE*,
and Woo-Young Choi, *Member, IEEE*

Abstract—We present a CMOS integrated optical receiver having under-damped transimpedance amplifier (TIA) and CMOS avalanche photodiode (APD) realized in 65-nm CMOS technology. The under-damped TIA compensates the bandwidth limitation of CMOS APD and provides enhanced receiver bandwidth performance with reduced power consumption and better sensitivity compared with previously reported techniques. We successfully demonstrate 10-Gb/s $2^{31}-1$ PRBS and 12.5-Gb/s 2^7-1 PRBS operation with the bit-error rate less than 10^{-12} at the incident optical power of -6 and -2 dBm, respectively. The receiver has core size of 0.24 mm \times 0.1 mm and power consumption excluding output buffer of ~ 13.7 mW with 1.2 V supply voltage.

Index Terms—CMOS PD, optical receiver, optoelectronic, transimpedance amplifier, under-damped response.

I. INTRODUCTION

AS THE bandwidth requirement for various interface applications continuously increases, there are growing research efforts for optical interconnects that can overcome the limitation of electrical interconnects. As one of these, 850-nm optical interconnects based on vertical-cavity surface-emitting lasers (VCSEL) and multimode fibers (MMF) are receiving much attention especially for such short-reach applications as chip-to-chip, board-to-board, or rack-to-rack interconnects [1]. For these applications, fully integrated 850-nm optical receivers implemented in standard complementary metal-oxide-semiconductor (CMOS) technology can provide great advantages in terms of fabrication cost and manufacturability [2], [3].

For CMOS integrated optical receivers, the bandwidth limitation of photodetectors (PDs) realized in standard CMOS PDs suffers from slow diffusive photocurrents. Although several high-speed monolithically integrated optical receivers realized in CMOS technology have been reported, they rely on either special PD structures such as spatially-modulated PDs (SM PDs) [4], [5] or electronic equalizers [6], [7]. However, SM PDs suffer from low responsivity and electronic equalizers require additional power and chip area. In this letter, we demonstrate a new and simple technique of

Manuscript received March 28, 2015; accepted April 6, 2015. Date of publication April 15, 2015; date of current version June 3, 2015. This work was supported by the National Research Foundation of Korea through the Korean Government within the Ministry of Education, Science and Technology under Grant 2012R1A2A1A-01009233. (Corresponding author: Woo-Young Choi.)

The authors are with the Department of Electrical and Electronic Engineering, Yonsei University, Seoul 120-749, Korea (e-mail: hyunghyung@gmail.com; sannmw@gmail.com; wchoi@yonsei.ac.kr).

Color versions of one or more of the figures in this letter are available online at <http://ieeexplore.ieee.org>.

Digital Object Identifier 10.1109/LPT.2015.2421501

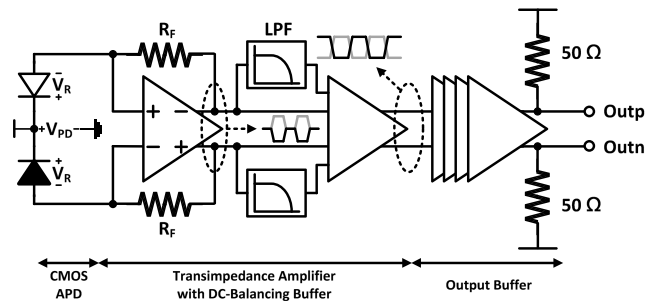


Fig. 1. Block diagram of the proposed optical receiver.

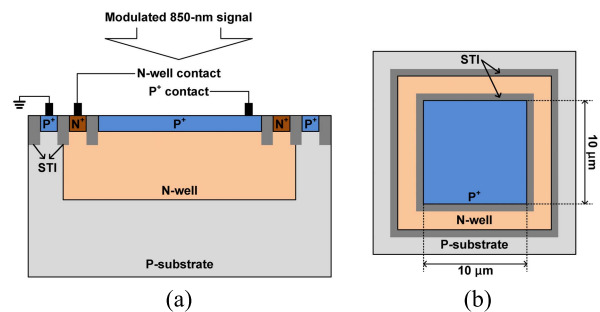


Fig. 2. (a) Cross section and (b) top view of the fabricated CMOS APD.

compensating PD bandwidth limit with an under-damped TIA which can have better power efficiency and small chip area.

II. CMOS INTEGRATED OPTICAL RECEIVER

Fig. 1 shows the simplified block diagram of our CMOS integrated optical receiver. It is composed of a CMOS APD with a dummy PD, an under-damped TIA with a DC-balancing buffer, and an output buffer with 50- Ω load. The dummy PD provides symmetric capacitance to the differential TIA input. Our receiver does not contain a limiting amplifier (LA) since we are interested in a fully integrated optical receiver in which PD, TIA and clock and data recovery (CDR) circuits are integrated together. Since typical CDR circuits require input voltage levels in the order of tens of mV, a LA is not needed if CDR circuit can be directly integrated with the TIA. The goal of this work is to verify the performance of PD and TIA before we can implement the fully integrated optical receiver.

A. CMOS Avalanche Photodiode

Fig. 2(a) and (b) show the cross-section and the top view of the CMOS APD used in our integrated receiver. It is realized with P^+ source/drain and N-well junction in standard CMOS technology without any design-rule violation.

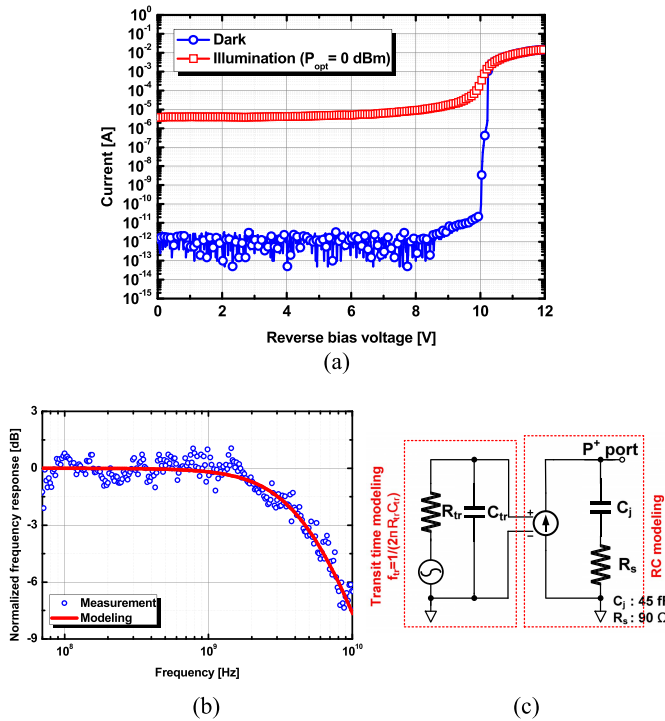


Fig. 3. (a) DC characteristic, (b) frequency response for measurement and model and (c) equivalent circuit model of CMOS APD.

Shallow trench isolation surrounding the vertical PN junction provides large and uniform electric fields that are desired for avalanche gain. Photo-generated currents are taken from P⁺ contact to TIA since currents from N-well include diffusive components due to light absorbed in P-substrate. The CMOS APD has 10 $\mu\text{m} \times 10 \mu\text{m}$ of optical-window for optimal photo-detection bandwidth [8].

For TIA design optimization, an accurate APD model is essential. The 3-dB bandwidth of our CMOS APD, f_{PD} , can be determined as $f_{PD} = 1/[(1/f_{tr})^2 + (1/f_{RC})^2]^{1/2}$ where f_{tr} and f_{RC} represent the 3-dB bandwidth due to photogenerated hole transit time and the APD RC time, respectively. Fig. 3(a) shows the measured DC characteristic of our APD with 0-dBm input optical power. For our optical receiver, the reverse bias voltage of 9.7 V is used, where the APD provides the best bit error rate (BER) performance as determined by measurement. Fig. 3(b) shows the measured photo-detection frequency response of our APD and Fig. 3(c) shows the equivalent circuit model of the APD. C_j and R_s represent the depletion region capacitance and N-well series resistance, respectively. R_{tr} and C_{tr} are used to model the influence of hole transit time in the APD. The numerical values of these parameters are determined by fitting equivalent circuit simulation results to measured s-parameter and frequency responses of CMOS APD. As can be seen in Fig. 3(b), the APD has limited 3-dB bandwidth of about 4.7 GHz.

B. Under-Damped TIA

The limited bandwidth of CMOS APD can be compensated by an under-damped TIA, which gives peaked frequency

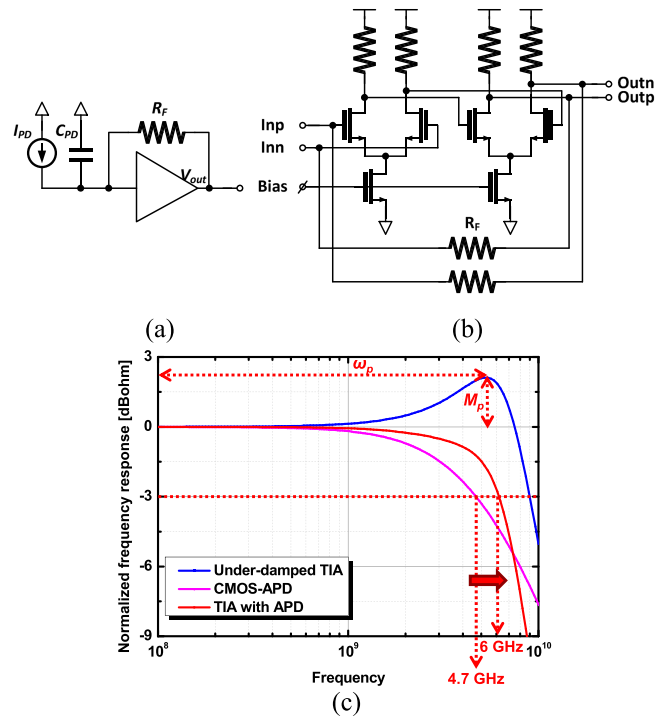


Fig. 4. (a) Block diagram, (b) schematic diagram and (c) simulated frequency response of the TIA.

response and, consequently, enhanced optical receiver bandwidth.

Fig. 4(a) shows the block diagram of our under-damped TIA. The shunt-shunt feedback configuration is used, which provides low noise characteristics and high gain-bandwidth product. Since the transfer function of the core voltage amplifier can be approximated as [9]

$$A(s) = \frac{A_0}{1 + s/\omega_0}, \quad (1)$$

the closed loop transfer function of the TIA is given as

$$\frac{V_{out}}{I_{PD}} = -\frac{A_0\omega_0}{C_{PD}} \frac{1}{s^2 + \frac{R_F C_{PD} + 1/\omega_0}{R_F C_{PD}} s + \frac{(A_0 + 1)\omega_0}{R_F C_{PD}}}, \quad (2)$$

which results in low-frequency transimpedance gain of $A_0 R_F / (A_0 + 1)$. The denominator of above equation can be expressed as the standard second-order system function as $s^2 + 2\zeta\omega_n s + \omega_n^2$, where ζ is the damping factor and ω_n is the natural frequency with [9]

$$\zeta = \frac{1}{2} \frac{R_F C_{PD} \omega_0 + 1}{\sqrt{(A_0 + 1)\omega_0 R_F C_{PD}}} \quad \text{and} \quad (3)$$

$$\omega_n = \sqrt{\frac{(A_0 + 1)\omega_0}{R_F C_{PD}}}. \quad (4)$$

The limited bandwidth of CMOS APD can be compensated by the peaked response of the under-damped TIA. For the under-damped response, we need $\zeta < \sqrt{2}/2$ and the peaking magnitude, M_p , and the peaking frequency, ω_p , are given as [10]

$$M_p = \frac{1}{2\zeta\sqrt{1 - \zeta^2}} \quad \text{and} \quad (5)$$

$$\omega_p = \omega_n \sqrt{1 - 2\zeta^2}, \quad (6)$$

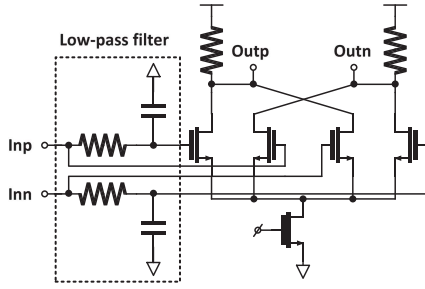


Fig. 5. Schematic diagram of the DC-balancing buffer.

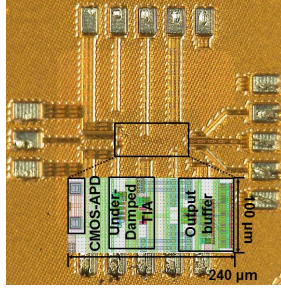


Fig. 6. Microphotograph and layout of the fabricated optical receiver.

M_p and ω_p should be carefully determined so that the limited bandwidth of CMOS APD can be effectively compensated. Fig. 4(b) presents the schematic diagram of our TIA and Fig. 4(c) shows the simulated frequency response of CMOS APD, under-damped TIA and the integrated optical receiver. The under-damped TIA used for simulation has 2-k Ω feedback resistor and core amplifier which provides 20-dB gain and 4.5-GHz bandwidth. The under-damped TIA results in 3.5 dB of M_p and 25 GHz of ω_p , which gives the optimal frequency compensation performance. As shown in the Figure 4(c), the under-damped TIA achieves 3-dB bandwidth of 6 GHz with a CMOS APD having 4.7-GHz bandwidth. It should be noted that this enhancement is achieved without any additional active circuits consuming additional power or SM PD decreasing responsivity only with TIA design modification.

C. DC-Balancing Buffer and Output Buffer

Delivering photo-generated currents to only one port of two differential TIA input ports induces a DC offset in TIA differential output, which can result bit errors with the decision threshold problem. To solve this problem, a DC-balancing buffer is added. Fig. 5 shows the schematic diagram of the designed DC-balancing buffer. Two on-chip low-pass filters and f_T -doubler are used, and to avoid any DC-wander effect, the low cut-off frequency is set to 1 MHz. Output buffers are designed so that they can deliver 200-mV_{peak-peak} swing to the 50- Ω load of the measurement equipment.

III. MEASUREMENT RESULTS

Fig. 6 shows the micro photograph and layout of the fabricated optical receiver. The core size is 0.24 \times 0.1 mm²,

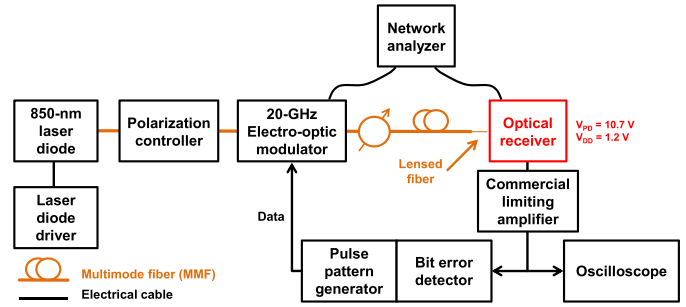


Fig. 7. Measurement setup.

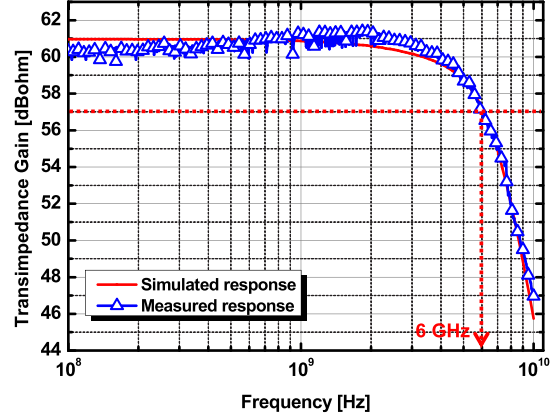


Fig. 8. Measured and simulated frequency response.

and the power consumption of the receiver excluding the output buffer is 13.7 mW with 1.2-V supply voltage.

Fig. 7 shows the measurement setup for photo-detection frequency response and optical data detection. All experiments are done on-wafer. The 850-nm modulated optical signals are generated by an 850-nm laser diode and a 20-GHz external electro-optic modulator. The modulated optical signals are injected into the optical receiver with lensed fiber. For measurement, V_{PD} of 10.7 V is used, which provides the optimal reverse bias voltage of 9.7 V to the CMOS APD. For BER evaluation, a 12.5-Gb/s commercial limiting amplifier is used in order to satisfy the input sensitivity requirement of our equipment.

Fig. 8 shows the measured and simulated photo-detection frequency responses. The transimpedance gain and 3-dB bandwidth is about 60 dB Ω and 6 GHz, and measured response is well matched with simulated response.

Fig. 9 shows the measured BER performances for 10- and 12.5-Gb/s input data. For 10 Gb/s, BER of 10⁻¹² is achieved with -6-dBm incident optical power for 2³¹-1 PRBS input data and -6.5 dBm for 2⁷-1 PRBS data. For 12.5 Gb/s, BER of 10⁻¹² and 10⁻¹¹ are achieved with -2-dBm incident optical power for 2³¹-1 and 2⁷-1 PRBS input data. Inset of Fig. 9 shows measured eye diagrams for 10- and 12.5-Gb/s data transmission with -6- and -2-dBm input power. Table I shows the performance comparison of our optical receiver with previously reported CMOS integrated optical receivers. The table also contains a column, which includes the power consumption and chip area of a LA having 0.076-mm² chip area, 38.4-mW power consumption,

TABLE I
PERFORMANCE COMPARISON OF THE REPORTED CMOS OPTICAL RECEIVERS

	[4] 11' JSSC	[7] 12' JQE	[5] 14' OE	This work	Estimated work
Technology	180-nm CMOS	130-nm CMOS	130-nm CMOS	65-nm CMOS	65-nm CMOS
Structure	*SM-PD + TIA + LA (Inductors)	APD + TIA + **EQ + LA	*SM-APD + TIA + **EQ + LA	APD + TIA (No LA)	APD + TIA + LA (LA is assumed)
Gain (dBΩ)	88	100	104	60	100
Bandwidth (GHz)	5.8	6	8	6	6
Data rate (Gb/s)	10	10	12.5	12.5	10
BER (PRBS)	10^{-11} (2^7-1)	10^{-12} (2^7-1)	10^{-12} (2^7-1)	10^{-12} (2^7-1)	10^{-12} ($2^{31}-1$)
Sensitivity	-6 dBm	-4 dBm	0 dBm	-2 dBm	-6 dBm
Supply voltage	1.8 V (Circuit) 14.2 V (PD)	1.2 V (Circuit) 10.5 V (PD)	1.3 V (Circuit) 10.5 V (PD)	1.2 V (Circuit) 10.7 V (PD)	1.2 V (Circuit) 10.7 V (PD)
Power	118 mW	66.8 mW	72.4 mW	13.7 mW	52.1 mW
Chip area	0.76 mm ²	0.26 mm ²	0.26 mm ²	0.024 mm ²	0.1 mm ²
***GB/P (Ω/mW)	1235	8982	17512	438	11516
Power efficiency (mW/Gb/s)	11.8	6.68	5.79	1.10	1.37

*SM PD: spatially-modulated photodetector, **EQ: equalizer, ***GB/P = gain×bandwidth/power dissipation

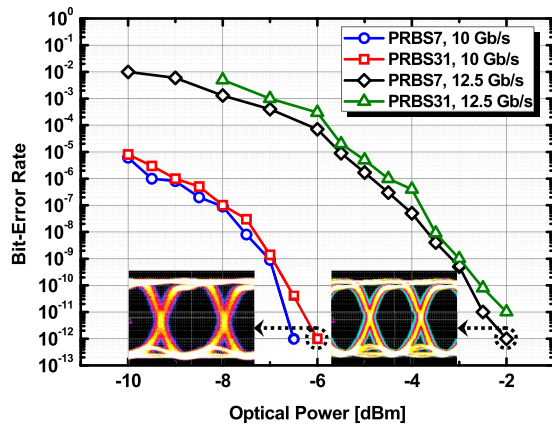


Fig. 9. Measured BER performances with various incident optical power 10- and 12.5-Gb/s data.

20-dB voltage gain and 12.5-GHz bandwidth [7] so that our optical receiver performance can be fairly compared with others. Two different types of figure of merit (FoM) are used in the table. For FoM of gain-bandwidth product per power, our integrated receiver without the LA shows inferior performance. This is due to the fact the LA provides most of the gain. This is needed when the output signals are delivered outside the circuit, but if the optical receiver is fully integrated including CDR circuits, then LA providing high gain is not necessary. For such an application, FoM for power efficiency defined as mW per Gb/s becomes more relevant. Chip area is another important factor for integrated solutions. For our integrated receiver application that does not require a LA. For this FoM, our receiver achieves the lowest value of 1.10. The power efficiency FoM becomes 4.17 if we include above-mentioned LA.

IV. CONCLUSION

A high-speed CMOS integrated optical receiver in which an under-damped TIA compensates the CMOS APD bandwidth limitation is realized in 65-nm CMOS technology. With precise CMOS-APD modeling and careful design of the under-damped TIA, the bandwidth enhancement can be achieved

without any additional equalizing circuits or SM PDs. Also, optical data up to 12.5 Gb/s are successfully detected by our integrated optical receiver. The design strategy employed in our receiver should be valuable for various high-performance electronic-photonic integrated circuit applications, in which careful design of both electronic circuits and photonic devices in an integrated manner can provide better performances with less power consumption and smaller system sizes.

ACKNOWLEDGMENT

The authors are very thankful to IC Design Education Center (IDEC) for MPW and EDA software support.

REFERENCES

- [1] T. K. Woodward and A. V. Krishnamoorthy, "1-Gb/s integrated optical detectors and receivers in commercial CMOS technologies," *IEEE J. Sel. Topics Quantum Electron.*, vol. 5, no. 2, pp. 146–156, Mar./Apr. 1999.
- [2] N. Bamiedakis, J. Beals, R. V. Pentyl, I. H. White, J. V. DeGroot, and T. V. Clapp, "Cost-effective multimode polymer waveguides for high-speed on-board optical interconnects," *IEEE J. Quantum Electron.*, vol. 45, no. 4, pp. 415–424, Apr. 2009.
- [3] L. Schares *et al.*, "Terabus: Terabit/second-class card-level optical interconnect technologies," *IEEE J. Sel. Topics Quantum Electron.*, vol. 12, no. 5, pp. 1032–1044, Sep./Oct. 2006.
- [4] S.-H. Huang, W.-Z. Chen, Y.-W. Chang, and Y.-T. Huang, "A 10-Gb/s OEIC with meshed spatially-modulated photo detector in 0.18- μ m CMOS technology," *IEEE J. Solid-State Circuits*, vol. 46, no. 5, pp. 1158–1169, May 2011.
- [5] M.-J. Lee, J.-S. Youn, K.-Y. Park, and W.-Y. Choi, "A fully-integrated 12.5-Gb/s 850-nm CMOS optical receiver based on a spatially-modulated avalanche photodetector," *Opt. Exp.*, vol. 22, no. 3, pp. 2511–2518, Feb. 2014.
- [6] D. Lee, J. Han, G. Han, and S. M. Park, "An 8.5-Gb/s fully integrated CMOS optoelectronic receiver using slope-detection adaptive equalizer," *IEEE J. Solid-State Circuits*, vol. 45, no. 12, pp. 2861–2873, Dec. 2010.
- [7] J.-S. Youn, M.-J. Lee, K.-Y. Park, and W.-Y. Choi, "10-Gb/s 850-nm CMOS OEIC receiver with a silicon avalanche photodetector," *IEEE J. Quantum Electron.*, vol. 48, no. 2, pp. 229–236, Feb. 2012.
- [8] M.-J. Lee and W.-Y. Choi, "Area-dependent photodetection frequency response characterization of silicon avalanche photodetectors fabricated with standard CMOS technology," *IEEE Trans. Electron Devices*, vol. 60, no. 3, pp. 998–1004, Mar. 2013.
- [9] B. Razavi, *Design of Integrated Circuits for Optical Communications*. New York, NY, USA: McGraw-Hill, 2002, pp. 89–91.
- [10] A. S. Sedra and K. C. Smith, *Microelectronic Circuits*, 4th ed. New York, NY, USA: Oxford Univ. Press, 1998, pp. 901–909.